




# Mouse dendritic cells in the steady state: Hypoxia, autophagy, and stem cell factor

Amarelys Belen Barroeta Seijas<sup>1</sup>  | Sonia Simonetti<sup>1</sup> | Irene Filippi<sup>2</sup> | Antonella Naldini<sup>2</sup> | Gabriele Favaretto<sup>1</sup> | Teresa Colombo<sup>1</sup> | Ambra Natalini<sup>1</sup> | Fabrizio Antonangeli<sup>1</sup> | Mattia Laffranchi<sup>3</sup>  | Silvano Sozzani<sup>3</sup> | Angela Santoni<sup>4,5</sup> | Francesca Di Rosa<sup>1</sup> 

<sup>1</sup>Institute of Molecular Biology and Pathology, National Research Council (CNR), Rome, Italy

<sup>2</sup>Department of Molecular and Developmental Medicine, University of Siena, Siena, Italy

<sup>3</sup>Department of Molecular Medicine, Sapienza University, Rome, Italy

<sup>4</sup>Neuromed IRCCS, Pozzilli, Isernia, Italy

<sup>5</sup>Istituto Pasteur Italia—Fondazione Cenci Bolognetti, Rome, Italy

## Correspondence

Francesca Di Rosa, Institute of Molecular Biology and Pathology, National Research Council (CNR), Rome, Italy, c/o Department of Molecular Medicine, Sapienza University, viale Regina Elena 291, 00161, Rome, Italy.  
Email: [francesca.dirosa@cnr.it](mailto:francesca.dirosa@cnr.it)

## Present address

Sonia Simonetti, Translational Oncology Laboratory, Campus Bio-Medico University, Rome, Italy.

Ambra Natalini, The Francis Crick Institute, London, UK.

## Funding information

Associazione Italiana per la Ricerca sul Cancro; Italian Minister of Research and University (MIUR) grant PRIN 2017K55HLC; CNR Short Term Mobility (STM)

## Abstract

Dendritic cells (DCs) are innate immune cells with a central role in immunity and tolerance. Under steady-state, DCs are scattered in tissues as resting cells. Upon infection or injury, DCs get activated and acquire the full capacity to prime antigen-specific CD4<sup>+</sup> and CD8<sup>+</sup> T cells, thus bridging innate and adaptive immunity. By secreting different sets of cytokines and chemokines, DCs orchestrate diverse types of immune responses, from a classical proinflammatory to an alternative pro-repair one. DCs are highly heterogeneous, and physiological differences in tissue microenvironments greatly contribute to variations in DC phenotype. Oxygen tension is normally low in some lymphoid areas, including bone marrow (BM) hematopoietic niches; nevertheless, the possible impact of tissue hypoxia on DC physiology has been poorly investigated. We assessed whether DCs are hypoxic in BM and spleen, by staining for hypoxia-inducible-factor-1 $\alpha$  subunit (HIF-1 $\alpha$ ), the master regulator of hypoxia-induced response, and pimonidazole (PIM), a hypoxic marker, and by flow cytometric analysis. Indeed, we observed that mouse DCs have a hypoxic phenotype in spleen and BM, and showed some remarkable differences between DC subsets. Notably, DCs expressing membrane c-kit, the receptor for stem cell factor (SCF), had a higher PIM median fluorescence intensity (MFI) than c-kit<sup>-</sup> DCs, both in the spleen and in the BM. To determine whether SCF (a.k.a. kit ligand) has a role in DC hypoxia, we evaluated molecular pathways activated by SCF in c-kit<sup>+</sup> BM-derived DCs cultured in hypoxic conditions. Gene expression microarrays and gene set enrichment analysis supported the hypothesis that SCF had an impact on hypoxia response and inhibited autophagy-related gene sets. Our results suggest that hypoxic response and autophagy, and their modulation by SCF, can play a role in DC homeostasis at the steady state, in agreement with our previous findings on SCF's role in DC survival.

## KEYWORDS

bone marrow, c-kit, dendritic cells, hypoxia, stem cell factor

This is an open access article under the terms of the Creative Commons Attribution-NonCommercial-NoDerivs License, which permits use and distribution in any medium, provided the original work is properly cited, the use is non-commercial and no modifications or adaptations are made.

© 2022 The Authors. *Cell Biochemistry and Function* published by John Wiley & Sons Ltd.

## 1 | INTRODUCTION

Dendritic cells (DCs) are heterogeneous cells of the innate immune system, that play a central role in innate and adaptive immune responses. DCs are scattered in lymphoid and extra-lymphoid tissues, wherein they sense the surrounding environment via their membrane and cytoplasmic receptors (e.g., Toll-like receptors [TLRs], NOD-like receptors, RIG-I-like receptors, etc.), acting as sentinels of possible perturbations. In case of infection or tissue damage, ligands derived from pathogens and/or injured cells bind to their corresponding receptors expressed by DCs, thus inducing a switch of these cells from a resting to an activated state, a transition which is often called DC maturation.<sup>1</sup> Depending on the newly released ligand(s), and on pre-existing cues from the tissue environment, DCs change their surface marker expression, migratory capability, and functional state. The resulting DC phenotype can range from a classical proinflammatory to an alternative pro-repair one.<sup>2</sup> DCs orchestrate local and systemic immunity by means of a wide variety of cytokines and chemokines, and have a central role in antigen-specific priming of naïve CD4<sup>+</sup> and CD8<sup>+</sup> T cells, thus bridging innate and adaptive immunity.

The main DC subsets are classical or conventional DCs (cDCs), that are specialized in naïve T-cell priming, and plasmacytoid DCs (pDCs), that have the capacity to produce huge amount of type I IFN.<sup>3</sup> According to a widely accepted ontogeny-based classification, cDCs are divided in cDC1s and cDC2s.<sup>4</sup> Under steady-state in the mouse, cDCs are characterized by high major histocompatibility complex (MHC)-II and CD11c membrane expression, while pDCs express low MHC-II and intermediate levels of CD11c. Human DCs constitutively express MHC-II, while differences in membrane expression of CD11c together with a set of blood dendritic cell antigens (BDCA) distinguish pDCs and cDC subpopulations.<sup>3</sup> cDC1s express the chemokine receptor XCR1 in both mice and humans, and are characterized by the expression of CD8 $\alpha$  in the mouse and BDCA-3 (CD141) in humans; cDC2s express CD11b in the mouse and BDCA-1 (CD1c) in humans.<sup>3,4</sup> Additional DC subpopulations have been described, for example, cDC2As e cDC2Bs, which are defined in mice by the mutual exclusive expression of the transcription factors Tbx21 (also known as T-bet), and ROR- $\gamma$ t.<sup>5</sup> Tissue specialization greatly contributes to DC phenotype variation.<sup>6</sup>

Oxygen tension is recognized as one key difference among diverse physiological and pathological tissue environments. Normal oxygen tension is about 70–100 mmHg and 40–50 mmHg in arterial and venous blood, respectively. Notably, under physiological conditions, oxygen tension is below 10 mmHg in some lymphoid organ areas, including bone marrow (BM) hematopoietic niches.<sup>7–9</sup> Furthermore, oxygen tension is typically decreased in ischemic and necrotic lesions, inflamed tissues, and solid cancers.<sup>8,10</sup> It has been proposed that immune cell adaptations to tissue hypoxia have evolved to enable appropriate regulation of immunity and tolerance under diverse physiological and pathological conditions.<sup>11,12</sup> Hypoxia-induced response includes cell-type specific changes as well as metabolic reprogramming and autophagy, a highly regulated

degradation process involved in the homeostatic turn-over of cellular components.<sup>13</sup> Hypoxic tissue environments can be mimicked in vitro by cell exposure to reduced oxygen tensions. By these means, several reports have demonstrated that hypoxia promotes migratory and functional changes of DCs (reviewed in Bosco and Varesio<sup>14</sup>). Among others, hypoxia was shown to inhibit the maturation of human monocyte-derived DCs and to modulate chemokine receptor expression.<sup>15</sup>

The master regulator of cellular response to reduced oxygen tension is the transcription factor hypoxia-inducible-factor-1 (HIF-1).<sup>16,17</sup> HIF-1 is a heterodimer formed by HIF-1 $\alpha$  and HIF-1 $\beta$ , an inducible and constitutive protein, respectively.<sup>16,17</sup> In addition to the ubiquitously expressed HIF-1 $\alpha$ , two tissue-restricted isoforms, that is, HIF-2 $\alpha$  and HIF-3 $\alpha$ , have been identified.<sup>16</sup> HIF-1 activity is mostly dependent on the stability of the HIF-1 $\alpha$  protein, that under normoxia has an extremely short half-life, as it is rapidly degraded following hydroxylation by the prolyl hydroxylases (PHDs), ubiquitination by the von Hippel-Lindau (VHL) E3 ubiquitin ligase and subsequent proteosomal-mediated decay. Hypoxia inhibits PHDs, resulting in slower HIF-1 $\alpha$  degradation, and increased transcriptional activity of the HIF-1 $\alpha$ /HIF-1 $\beta$  heterodimer. Under physiological conditions, HIF-1 $\alpha$  is typically highly expressed by the hematopoietic stem and progenitor cells (HSPCs) in BM niches.<sup>18</sup> HIF-1 $\alpha$  is also upregulated by cancer cells in hypoxic tumor microenvironments.<sup>10</sup> HIF-1 drives the expression of genes relevant to erythropoiesis, glucose metabolism, angiogenesis, inflammatory response, cell recruitment to sites of injury, and so forth.<sup>16,19</sup> It should be noted that oxygen-independent stimuli, for example proinflammatory cytokines and the Gram-negative bacteria lipopolysaccharide (LPS), a TLR-4 ligand, can also activate HIF-1 $\alpha$  in innate immune cells,<sup>17,20,21</sup> while stem cell factor (SCF, also known as kit ligand) can induce HIF-1 $\alpha$  in hematopoietic stem cells (HSCs).<sup>22</sup> In respect to DCs, it has been shown that TLR engagement stabilizes HIF-1 $\alpha$  in mouse BM-derived DCs (BMdDCs) via a mechanism requiring MYD88-dependent NF- $\kappa$ B activation, in contrast to the hypoxia-mediated HIF-1 $\alpha$  stabilization, which was preserved in the absence of MYD88.<sup>23</sup> Furthermore, our previous work showed that short-term hypoxia modulated human monocyte-derived DC migration through HIF-1 $\alpha$  and PI3K/Akt pathway.<sup>24</sup>

It was previously observed that mouse BMdDCs comparably survived in vitro under either hypoxic or normoxic conditions<sup>25</sup>; nevertheless, the possibility that DCs have a physiological hypoxic metabolism and/or express HIF-1 $\alpha$  in vivo has not been investigated so far. Furthermore, we and others showed that spleen and BM DCs express c-kit (CD117), the receptor for SCF, and demonstrated the relevance of SCF in differentiated DC biology.<sup>26–30</sup> Even though it is well-known that c-kit is a tyrosine kinase receptor that upon SCF binding activates PI-3 kinase, PLC $\gamma$ , src-family kinases, and other intracellular signaling molecules,<sup>31,32</sup> the molecular pathways triggered by SCF in c-kit<sup>+</sup> DCs under hypoxic conditions which mimic those typical of some lymphoid niches<sup>8,9</sup> have not been investigated yet.

Here, we asked whether hypoxia and c-kit/SCF axis are intertwined in mouse DCs. We observed that DCs have a hypoxic

phenotype in physiological conditions in the spleen and BM, and showed remarkable differences between DC subsets. We also studied the molecular pathways activated by SCF in c-kit<sup>+</sup> BMdDCs cultured in hypoxic conditions. We found that hypoxia response and autophagy pathways are modulated in the presence of SCF, with possible implications for DC maintenance and functionality.

## 2 | MATERIALS AND METHODS

### 2.1 | Mice and treatment

Female C57BL/6J (B6) mice were purchased from Charles River and housed at the animal facility of Istituto Superiore di Sanità of Rome (ISS), according to institutional guidelines (DL116/92 and 26/2014), under the Italian Ministry of Health authorization number 358/2018-PR. Untreated mice were euthanized for generation of BMdDCs, and for HIF-1 $\alpha$  staining experiments. For experiments with pimonidazole (PIM), mice were either injected intraperitoneally with PIM in PBS (125 mg/kg PIM) 3 h before euthanasia or left untreated.<sup>18,33</sup> Spleen and BM were obtained as we previously described.<sup>27</sup>

### 2.2 | Staining and flow cytometric analysis

Cell membrane staining of single-cell suspensions from spleen and BM was performed with fluorochrome-conjugated monoclonal antibodies (mAbs), after blocking with anti-Fc $\gamma$ R (clone 2.4G2) mAb. The following mAbs were used (clone indicated in parentheses): anti-CD11c phycoerythrin (PE) (HL3), anti-I-Ab or MHC-II PE-Cy7 (M5/114.15.2), anti-c-kit APC (2B8), Ly-6A or Sca-1 APC-Cy7 (D7), Ly-6G or Gr-1 peridinin chlorophyll protein (PerCP)-Cy5.5 (RB6-8C5), B220 PerCP-Cy5.5 (RA3-6B2), Ter-119 PerCP-Cy5.5 (Ter-119), CD3 PerCP-Cy5.5 (145-2C11) (all from BD Biosciences; Biolegend; eBioscience). Dead cells were excluded with propidium iodide (PI, Sigma-Aldrich). For intracellular staining, cells were fixed, permeabilized, and stained using either anti-HIF-1 $\alpha$  (241812) or mouse IgG1 FITC (both from R&D). For PIM staining, HP-FITC-MAb was used (Hypoxyprobe Inc.). As a control, we used fluorescence minus one (FMO)-stained samples, that is, samples treated identically to the others but without HP-FITC-Mab. Samples were analyzed by FACSCanto II (BD Biosciences), and data were analyzed using FlowJo software, v.9.7.6 and 9.9.6 (FlowJo).

### 2.3 | Pathways enrichment analysis of publicly available bulk RNAseq data of mouse spleen DCs

RNAseq data from mouse spleen DCs were downloaded from GEO (GSE130201)<sup>5</sup> and normalized by DESeq2 method. Pathway enrichment analysis was performed by using the gene set enrichment analysis (GSEA) approach. To this end, we used the GSEA software (release 4.1.0) that is freely available online at <https://www.gsea->

[msigdb.org/gsea/](https://www.gsea-msigdb.org/gsea/) as well as Gene Sets obtained from selected Gene Ontology (GO) annotations of mouse genes, and formatted according to the GSEA software manual (<https://www.gsea-msigdb.org/gsea/doc/GSEAUUserGuideFrame.html>) (Supporting Information: Table S1). Differences were considered significant when the false discovery rate (FDR) < 0.25.

### 2.4 | Clustering of publicly available single-cell RNA seq (scRNAseq) data and analysis of Kit<sup>+</sup> mouse spleen cDC1s

Raw counts from publicly available scRNAseq experiments performed with mouse spleen DCs were downloaded from GEO (GSE137710)<sup>5</sup> and processed with the R package. Seurat v4.05 was used under RStudio v4.1.5.<sup>34</sup> In detail, we cleaned the data set by removing cells with a gene number <200 and a mitochondrial gene ratio  $\geq 25\%$ . Since the data set was sequenced in several cartridges, we merged their data set with the Seurat “integration” function<sup>35</sup> and with “SCTransform” for normalization and data scaling.<sup>36</sup> Highly variable genes (HVG,  $n = 3000$ ) were also identified with the “SCTransform” function. The HVGs were used as input for principal component analysis (PCA). The first 30 PCAs were utilized in the subsequent analysis. Cells were then embedded by Uniform Manifold Approximation and Projection (UMAP) plot and clustered with a resolution of 0.7. We applied the “FindAllMarkers” to identify differentially expressed genes (DEGs) among all genes by using the Wilcoxon rank sum test. To assign cDC1, cDC2, and monocyte identities, we referred to the original cell types from Brown et al.<sup>5</sup> We selected only genes that showed: (1) a minimal expression (min.pct  $\geq 2\%$ ) in at least one cluster; (2) an adjusted  $p \leq .05$ ; (3) an average log<sub>2</sub>-fold change (logFC)  $\geq 0.2$ . Genes marking the Kit<sup>+</sup> cDC1c cluster were analyzed with the tool g:Profiler,<sup>37</sup> after removing genes coding for ribosomal proteins and pseudogenes (Supporting Information: Table S2).

### 2.5 | BMdDCs stimulation with SCF under hypoxia

We generated DCs from BM cells of untreated B6 mice as previously described.<sup>27</sup> Briefly, 10–15  $\times 10^6$  BM cells were cultured for 1 week in an incubator at 37°C in normoxia (21% O<sub>2</sub>) in RPMI Medium 1640 (Sigma-Aldrich) supplemented with glutamine, penicillin/streptomycin, 50  $\mu$ M  $\beta$ -mercaptoethanol, 10% heat-inactivated fetal calf serum (FCS) and 20 ng/ml GM-CSF (BD Falcon, BD Biosciences). Non-adherent and slightly adherent cells were collected and CD11c<sup>+</sup> cells were purified with anti-CD11c magnetic microbeads (Miltenyi Biotec), thus obtaining BMdDCs (~98% CD11c<sup>+</sup>). BMdDCs were cultured for 2 days in workstation InVIVO2 400 (Ruskin) at 37°C in hypoxia (2% O<sub>2</sub>, ~14 mmHg)<sup>24</sup> in Opti-MEM medium supplemented with glutamine, penicillin/streptomycin, 50  $\mu$ M  $\beta$ -mercaptoethanol, and 20 ng/ml GM-CSF, and then either treated for 6 h with recombinant SCF (Immunotools) at 100 ng/ml or left untreated. Cells

were kept in hypoxic workstation and never exposed to normal air till the end of the experiment.

## 2.6 | Gene expression microarrays and pathways enrichment analysis of BMdDCs

BMdDCs stimulated or not with SCF as above were harvested and centrifuged. For each condition,  $2 \times 10^6$  BMdDCs were resuspended in 1 ml TRI-reagent (Sigma-Aldrich). Total RNA was extracted following the Qiagen RNeasy (Qiagen) clean-up procedure. Gene expression was evaluated by Affimetrix GeneChip Array (mogene 2.1 ST array strip) by Transcriptomics Platform, Department of Medicine and Surgery, University of Milano-Bicocca (TP Bicocca). Arrays were preprocessed and expression levels normalized across samples by using the Robust Multichip Average (RMA) method by TP Bicocca. Pathway enrichment analysis was performed by using the GSEA software as above, together with microarray gene annotations available from NCBI's GEO (<https://www.ncbi.nlm.nih.gov/geo/query/acc.cgi?acc=GPL17400>) (Supporting Information: Table S3).

## 2.7 | Statistics

We performed a two-tailed Student's *t* test (two groups) and ANOVA test (>two groups) using Prism v.6.0, GraphPad Software. Differences were considered significant when  $*p \leq .05$ ,  $**p \leq .01$ ,  $***p \leq .001$ .

## 3 | RESULTS

### 3.1 | DCs in spleen and BM express HIF-1 $\alpha$

We performed flow cytometric analysis of HIF-1 $\alpha$  expression by the spleen and BM DCs obtained from untreated C57BL/6/J (B6) mice. We focused our analysis on CD11c<sup>hi</sup> MHC-II<sup>hi</sup> DCs, which typically include cDCs but not pDCs.<sup>3</sup> Examples of HIF-1 $\alpha$  histograms are shown in Figure 1A,B. As a positive control, in each sample, we analyzed BM CD11c<sup>-</sup> c-kit<sup>hi</sup> cells, that are enriched in HSPCs, a cell population known to highly express HIF-1 $\alpha$ <sup>18</sup> (representative example in Figure 1C). We found that HIF-1 $\alpha$  median fluorescence intensity (MFI) was significantly higher within spleen DCs than within the total of spleen cells (Figure 1D). Similarly, BM DCs had a significantly higher HIF-1 $\alpha$  expression than total BM cells (Figure 1E). Notably, HIF-1 $\alpha$  MFI of spleen DCs and BM DCs were in the same range, being on the average 1045 and 1004, respectively, and only slightly lower than HIF-1 $\alpha$  MFI of HSPCs (Figure 1D,E). Supporting Information: Figure S1 shows our gating strategy for DC flow cytometric analysis (Supporting Information: Figure S1A,B), and confirms that in our hands, BM Lin<sup>-</sup> c-kit<sup>hi</sup> Sca-1<sup>-</sup> cells (BM LK<sup>+</sup>S<sup>-</sup>, a phenotypically defined population of HSCs) contained a high proportion of HIF-1 $\alpha$ <sup>+</sup> cells (Supporting Information: Figure S1C,D), in agreement with previous findings.<sup>18</sup> Altogether, these results show

that DCs in spleen and BM express HIF-1 $\alpha$  at a much higher level than total cells in the same organ, thus resembling BM HSCs in the BM.

### 3.2 | DCs in the spleen and BM have a hypoxic phenotype

To investigate whether spleen and BM DCs have a hypoxic phenotype *in vivo*, we took advantage of pimonidazole (PIM), a drug forming intracellular adducts in conditions of low oxygen tension and hypoxic metabolism, that can then be detected by a specific anti-PIM mAb.<sup>18,33</sup> We treated mice with 125 mg/kg PIM, and after 3 h analyzed DCs from the spleen and BM, and HSPCs. Untreated mice were analyzed in parallel as a control. PIM treatment did not cause any significant change in the percentage of spleen DCs (Supporting Information: Figure S2A), nor in that of BM DCs (Supporting Information: Figure S2B). Similarly, CD11c MFI and MHC-II MFI were comparable between DCs from PIM-treated mice and DCs from untreated mice, both in the spleen (Supporting Information: - Figure S2C) and in the BM (Supporting Information: Figure S2D). Independently of PIM treatment, MHC-II MFI was higher in BM DCs than in spleen DCs, in agreement with previous studies by us and others.<sup>27,38</sup> PIM assay specificity was reflected by a statistically significant increase of PIM mAb MFI in PIM-injected mice compared with untreated mice, even though some background staining was detected in untreated mice. Specifically, PIM MFI mean  $\pm$  SD values of three untreated and six PIM-injected mice were, respectively: spleen DCs  $1205 \pm 59$  and  $2923 \pm 300$  ( $p \leq .01$ ); BM DCs  $1453 \pm 88$  and  $3199 \pm 340$  ( $p \leq .01$ ); and BM HSPCs  $2861 \pm 181$  and  $6233 \pm 795$  ( $p \leq .01$ ). Examples of PIM histograms are shown in Figure 2A. As summarized in Figure 2B, we found that PIM mAb MFI of spleen DCs from PIM-injected mice was significantly higher than that of total spleen cells from the same mice. Similarly, BM DCs had a significantly higher PIM mAb MFI than BM total cells (Figure 2C). We used HSPCs from BM as a positive control,<sup>18</sup> and observed that PIM mAb staining was on average twofold higher in HSPCs than in BM DCs (Figure 2C). Taken together, our results on HIF-1 $\alpha$  and PIM suggest that DCs in the spleen and BM have a hypoxic phenotype under steady-state conditions, and express higher levels of HIF-1 $\alpha$  than the total cells in the same organ.

### 3.3 | Spleen and BM DC heterogeneity with respect to hypoxia

Beyond the widely accepted division of cDCs into the two main subsets, cDC1 and cDC2,<sup>4</sup> novel experimental approaches have enabled the discovery of further subpopulations, especially among cDC2s.<sup>5,6</sup> Brown et al.<sup>5</sup> exploited T-bet reporter mice and performed transcriptional and chromatin analysis to dissect mouse spleen DC heterogeneity. These authors identified two new cDC2 subsets, so-called cDC2A and cDC2B, with anti-inflammatory and proinflammatory profiles, respectively.<sup>5</sup>

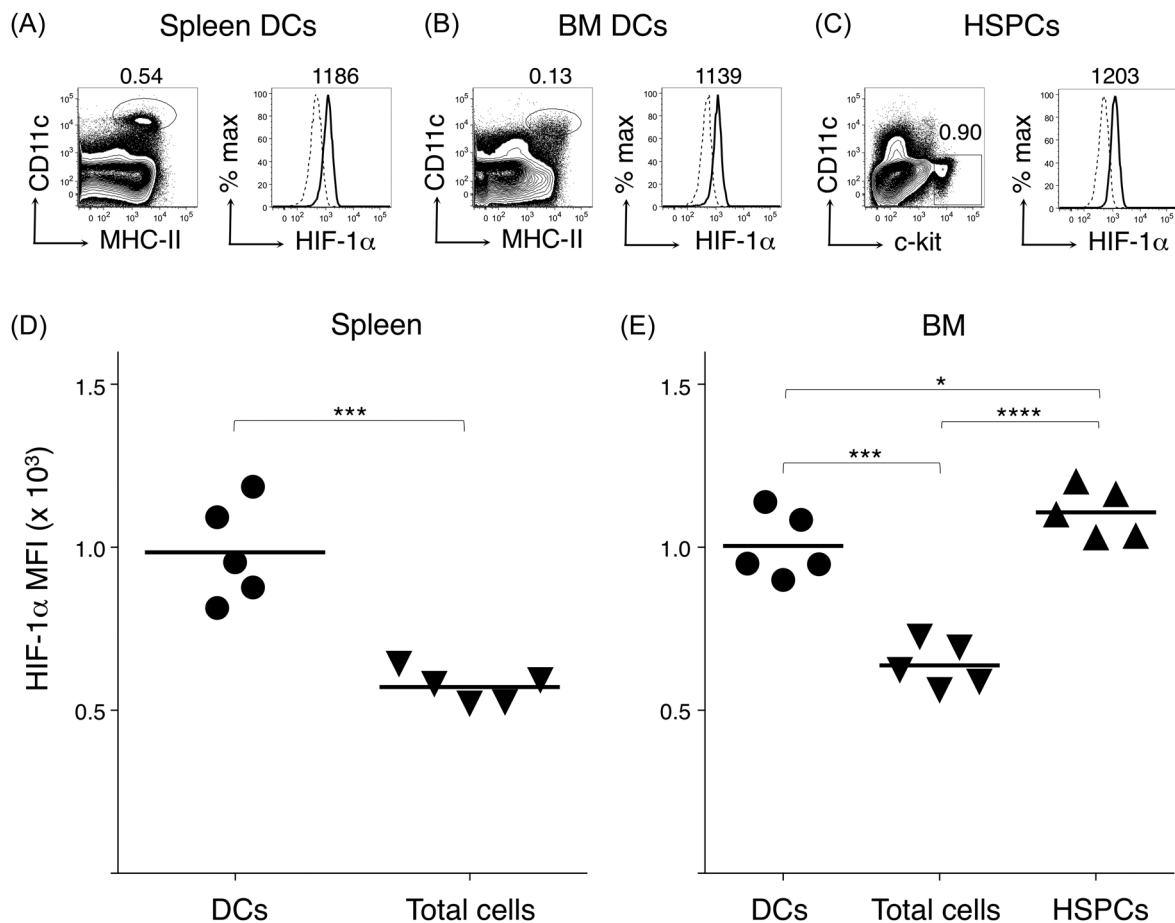


**FIGURE 1** HIF-1 $\alpha$  expression by mouse spleen and BM DCs. Spleen and BM cells were obtained from untreated B6 mice. After staining with fluorochrome-conjugated mAbs, cells were analyzed by flow cytometry (for gating strategy see Supporting Information: Figure S1). (A–C) Representative examples of flow cytometric profiles of CD11c<sup>hi</sup> MHC-II<sup>hi</sup> spleen DCs (A), CD11c<sup>hi</sup> MHC-II<sup>hi</sup> BM DCs (B), and CD11c<sup>–</sup> c-kit<sup>hi</sup> HSPCs (C), gated as indicated; numbers above plots represent percentages of cells in the indicated regions. Histograms show HIF-1 $\alpha$  staining profiles (solid line) and corresponding isotype controls (dashed line); numbers above histograms represent MFI of HIF-1 $\alpha$  staining. D, E Summary of HIF-1 $\alpha$  results. Individual mice from two independent experiments and mean values (bar) are shown ( $n = 5$ ). BM, bone marrow; DC, dendritic cells; MFI, median fluorescence intensity.

cDC2As expressed Tbx21 (alias T-bet), while cDC2Bs did not, and were positive for ROR- $\gamma$ t expression.<sup>5</sup> We used the publicly available bulk RNA sequencing (RNA-seq) data from the study by Brown and coworkers to evaluate the hypoxia-induced molecular pathway in mouse spleen cDC1s, cDC2As and cDC2Bs from *Tbx21*<sup>RFP-Cre</sup> mice.<sup>5</sup> Our comparison between cDC2As and cDC2Bs by GSEA<sup>39</sup> revealed that both the response to hypoxia gene set (gene set matching the GO term 0001666) and the cellular response to hypoxia gene set (GO term 0071456) had a statistically significant bias toward cDC2Bs, while a similar comparison between cDC2As and cDC1s revealed a slightly less pronounced but still significant bias toward cDC1s (Supporting Information: Figure S3, Table S1). No significant difference in the annotation of assayed genes to the biological process negative regulation of cellular response to hypoxia (GO term 1900038) was observed when comparing cDC2As and cDC2Bs, nor cDC2As and cDC1s. Furthermore, no significant difference in the annotation of assayed genes in the three gene sets above was observed between cDC2Bs and cDC1s (Supporting Information: Figure S3, Table S1).

Variation in c-kit expression contributes to mouse cDC heterogeneity,<sup>27,28</sup> while pDCs are negative for this receptor.<sup>3,40</sup> In agreement with our previous findings,<sup>27</sup> most spleen CD11c<sup>hi</sup> MHC-II<sup>hi</sup> DCs, and a minor fraction of BM CD11c<sup>hi</sup> MHC-II<sup>hi</sup> DCs expressed c-kit on their membrane (representative c-kit histograms in Figure 3A,B, left panels). We investigated whether DCs expressing c-kit in either spleen or BM had a different hypoxic phenotype than c-kit<sup>–</sup> DCs in the same organ. We observed that HIF-1 $\alpha$  expression was roughly similar in c-kit<sup>+</sup> and c-kit<sup>–</sup> DCs (examples of HIF-1 $\alpha$  histograms in Figure 3A,B, right panels). In contrast, we found that c-kit<sup>+</sup> DCs had a significantly higher PIM MFI than c-kit<sup>–</sup> DCs in PIM-injected mice (examples of PIM histograms in Figure 3C,D, and corresponding FMOs in Supporting Information: Figure S2C,D; summary of data in Figure 3E,F). On average, there was a ~1.6- and ~1.3-fold difference between c-kit<sup>+</sup> and c-kit<sup>–</sup> DCs in the spleen and BM, respectively (Figure 3E,F). In regard to spleen data, it should be noted that we previously showed by flow cytometry that cDC1s and

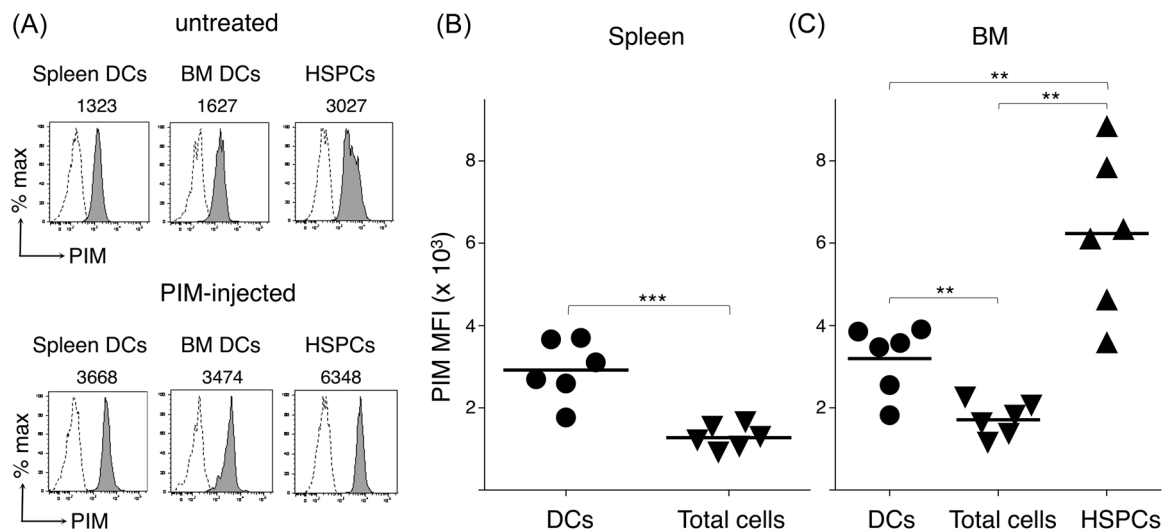


**FIGURE 2** Analysis of hypoxic phenotype of mouse spleen and BM DCs by PIM assay. B6 mice were either intraperitoneally injected with PIM (125 mg/kg) or left untreated. After 3 h, spleen and BM cells were purified, stained with fluorochrome-conjugated mAbs and analyzed by flow cytometry, after gating on spleen DCs, BM DCs, and HSPCs as in Figure 1. (A) Histograms show anti-PIM mAb staining profiles (gray-filled line) and corresponding FMO controls (dashed line) of cells obtained from typical untreated (top) and PIM-injected (bottom) mice, as indicated; numbers represent MFI of PIM-mAb staining. B, C Summary of PIM results from PIM-injected mice. Individual mice and mean values (bar) are shown. Mice were analyzed in three independent experiments; in each experiment up to four mice were examined (1 untreated and 1–3 PIM-injected;  $n = 9$ ). BM, bone marrow; DC, dendritic cells; FMO, fluorescence minus one; HSPCs, hematopoietic stem and progenitor cells; MFI, median fluorescence intensity; PIM, pimonidazole.

cDC2s have similar percentages of c-kit<sup>+</sup> cells.<sup>27</sup> Similarly, RNA-seq data from Brown et al.<sup>5</sup> did not reveal any significant difference among spleen cDC1, cDC2As, and cDC2Bs in terms of c-kit expression (c-kit mean  $\pm$  SD counts after DESeq2 normalization and log<sub>10</sub> transformation were  $3.99 \pm 0.25$ ,  $4.07 \pm 0.06$ , and  $4.02 \pm 0.15$ , respectively).

Notably, when we analyzed *Kit* (the gene coding for c-kit) expression by mouse spleen DCs in the publicly available single-cell RNAseq (scRNAseq) data from Brown and et al.,<sup>5</sup> we found that it was intertwined with the molecular pathways of response to hypoxia. In detail, within the UMAP, we identified only one *Kit*<sup>+</sup> cluster among 18 (Supporting Information: Figure S4A,B). This cluster expressed the cDC1 core signature cDC1 (i.e., *Xcr1*, *Clec9a*, *Cd8a*, *Irf8*, *Batf3*, *Cd207*), and was uniquely characterized by gene expression profiles involved in oxygen sensing and hypoxia, including the gene set matching the GO term response to hypoxia (GO 0001666) ((Supporting Information: Figure S4C, Table S2). Furthermore, this cluster (identified as “cDC1c”) showed a trend of positive *Hif1a* mRNA expression that did not reach statistical significance (Supporting Information: Figure S4B, Table S2).

It should be highlighted that RNAseq and scRNAseq data were obtained only with spleen DCs,<sup>5</sup> while we investigated in parallel spleen and BM DCs. Nevertheless, altogether, these results suggest that the hypoxic response pathway displays some diversities among spleen and BM DC subsets, possibly reflecting intrinsic differences in DC phenotypes or extrinsic signals from the microenvironment.

### 3.4 | Molecular pathways activated by SCF in BM-derived DCs (BMdDC) under hypoxia

To investigate SCF-triggered molecular pathways in hypoxic conditions, we firstly generated BMdDCs enriched in c-kit<sup>+</sup> cells according to our previous protocol.<sup>27,28</sup> In more detail, we cultured BM cells from B6 mice with GM-CSF in normoxia for 7 days, sorted them using CD11c-microbeads, and obtained ~98% pure CD11c<sup>+</sup> BMdDCs. We then cultured BMdDCs under hypoxic conditions (~14 mmHg O<sub>2</sub>) with GM-CSF at 20 ng/ml for 2 days and finally incubated them either in the presence or absence of SCF at 100 ng/ml for further 6 h. After RNA extraction, we evaluated gene expression by Affimatrix Genechip array. We analyzed the distribution of gene annotation to selected intracellular pathways with respect to gene expression changes induced by SCF treatment of BMdDCs in hypoxic conditions. We focused on genes involved in myeloid, mononuclear, and DC differentiation, activation, and response to cytokines, as well as on genes implicated in response to hypoxia and autophagy (Figure 4, Supporting Information: Table S3 and Section 2). We found that the GO term matching DC differentiation (GO term 0097028) had a statistically significant bias toward genes expressed at higher level in SCF-stimulated BMdDCs (Figure 4A,B). Notably, gene annotations to both the cellular response to hypoxia and the response to hypoxia (GO term 0071456 and 0001666, respectively) had a markedly and statistically significant bias toward genes expressed at higher level in untreated BMdDCs (Figure 4A,C,D).

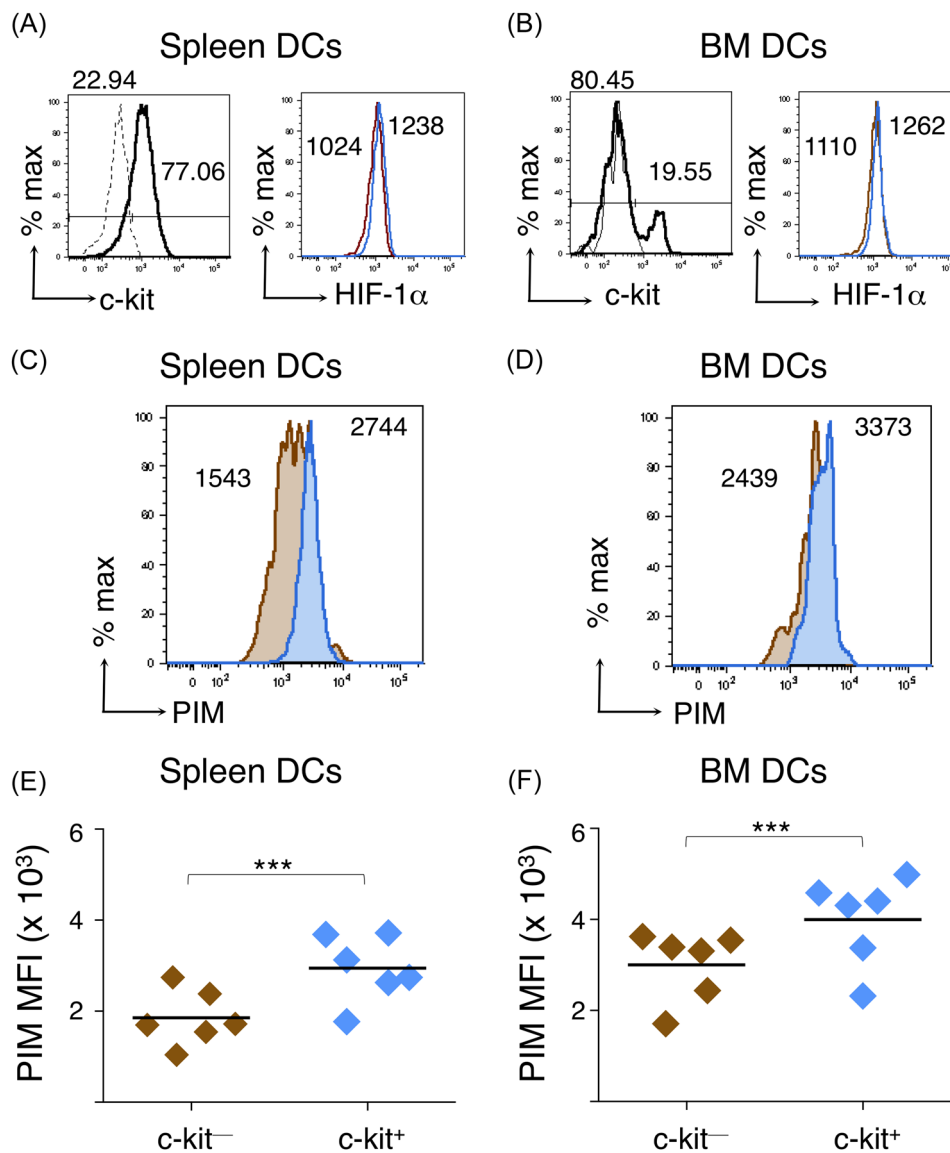


**FIGURE 3** HIF-1 $\alpha$  expression and PIM binding by c-kit<sup>+</sup> and c-kit<sup>-</sup> DCs from spleen and BM. A, B Spleen and BM cells were obtained from untreated B6 mice, stained and analyzed by flow cytometry as in Figure 1. Spleen DCs (A) and BM DCs (B) were gated as in Figure 1A, B, respectively. In left histograms, c-kit (solid line) and corresponding FMO control (dashed line) profiles are shown; numbers represent percentages of c-kit<sup>+</sup> and c-kit<sup>-</sup> cells in the indicated regions. In HIF-1 $\alpha$  histograms (right), c-kit<sup>+</sup> (blue line) and c-kit<sup>-</sup> (brown line) DCs are shown; numbers represent HIF-1 $\alpha$  MFI of c-kit<sup>+</sup> and c-kit<sup>-</sup> DCs. Each panel is a representative example of at least five mice. C–F Spleen and BM cells were obtained from PIM-injected B6 mice, stained and analyzed by flow cytometry as in this figure. Typical PIM histograms of spleen DCs (C) and BM DCs (D) showing c-kit<sup>+</sup> (blue-filled line) and c-kit<sup>-</sup> (brown-filled line) DCs; numbers represent PIM MFI of c-kit<sup>+</sup> and c-kit<sup>-</sup> DCs (corresponding FMO in Supporting Information: Figure S3E–F). Each panel is a representative example of at least six mice. Summary of PIM MFI of c-kit<sup>+</sup> and c-kit<sup>-</sup> spleen DCs (E) and BM DCs (F). Individual mice from three independent experiments and mean values (bar) are shown ( $n = 6$ ). BM, bone marrow; DC, dendritic cells; FMO, fluorescence minus one; HIF-1 $\alpha$ , hypoxia-inducible-factor-1; MFI, median fluorescence intensity; PIM, pimonidazole.

Moreover, several gene sets related to autophagy, that is, autophagy (GO term 0006914), autophagosome assembly (GO term 0000045), regulation of autophagy (GO term 0010506), and positive regulation of autophagy (GO term 0010508), were also significantly biased toward genes expressed at higher level in untreated BMdDCs (Figure 4A,E–G). These results suggest that SCF triggered-pathway might drift BMdDC phenotype away from autophagy, and modulate response to hypoxia.

## 4 | DISCUSSION

It is well-established that DCs are extremely heterogeneous, as, in fact, they comprise several different subsets, and can acquire a variety of functional states upon stimulation.<sup>3,4,6</sup> In our previous work, we showed that mouse and human cDCs differently express c-kit in distinct lymphoid organs.<sup>27</sup> Indeed, in both human and mouse BM, the percentage of c-kit<sup>+</sup> cells was about five times higher among

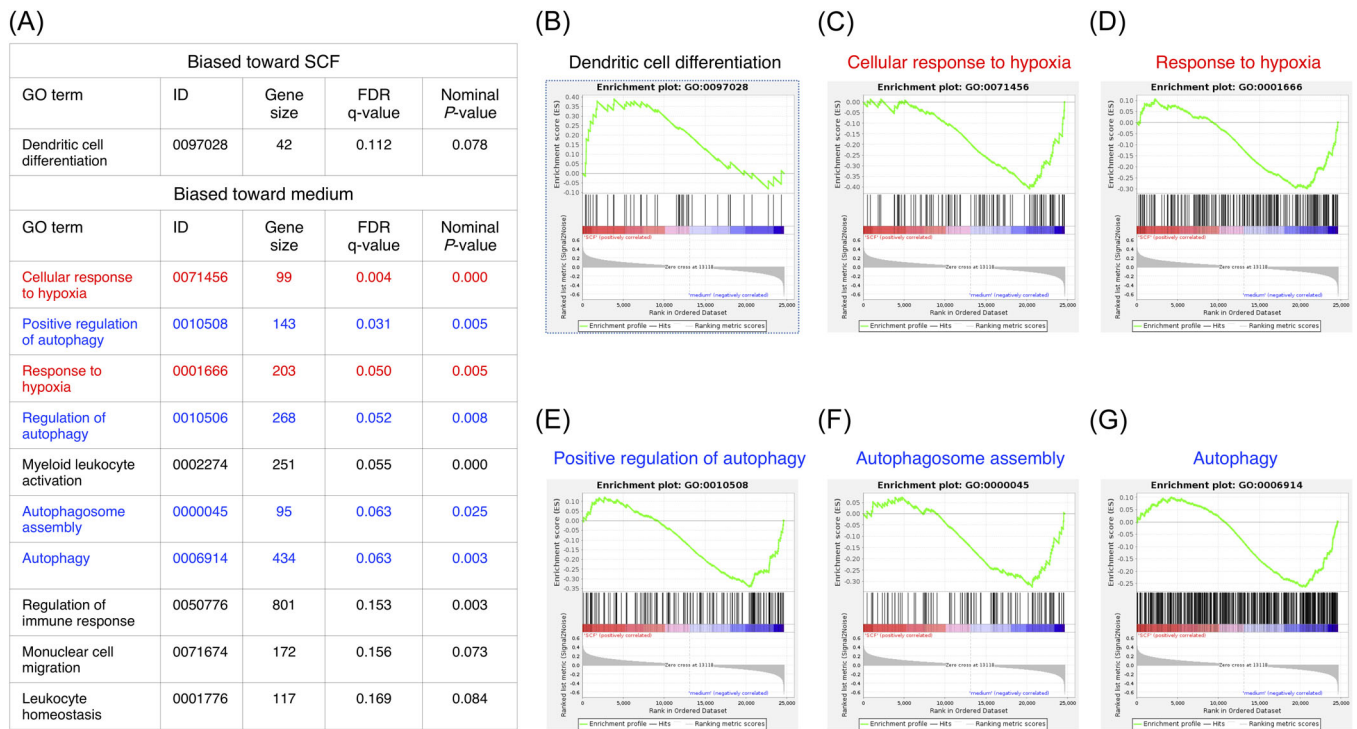


**FIGURE 4** GSEA of microarray data from mouse BMdDCs stimulated with SCF under hypoxia. BMdDCs enriched in c-kit<sup>+</sup> cells were generated according to our previous protocol,<sup>27,28</sup> cultured under hypoxia for 2 days, and then either stimulated with SCF at 100 ng/ml (SCF) or not (medium) for 6 h. After RNA extraction, gene expression was analyzed by Affimetrix microarray (medium vs. SCF comparisons from four experiments,  $n = 8$ ). Bioinformatic analysis was run by GSEA on data normalized by RMA method (Supporting Information: Table S3). A GO terms showing a statistically significant difference are listed (those involved in hypoxia and autophagy molecular pathways are indicated in red and blue, respectively). B Dendritic cell differentiation gene set (GO term 0097028). C Cellular response to hypoxia gene set (GO term 0071456). D Response to hypoxia gene set (GO term 0001666). E Positive regulation of autophagy gene set (GO term 0010508). F Autophagosome assembly gene set (GO term 0000045). G Autophagy gene set (GO term 0006914). BM, bone marrow; BMdDC, BM-derived DCs; DC, dendritic cells; GO, Gene Ontology; GSEA, gene set enrichment analysis; RMA, Robust Multichip Average; SCF, stem cell factor.

cDC1s than among cDC2s, while in mouse spleen most cDC1s and cDC2s expressed c-kit, without significant differences between the two subsets.<sup>27</sup> In respect to DC biology, some studies showed that SCF/c-kit was involved in the regulation of Th2 responses,<sup>26,29</sup> while we implicated this pathway in DC survival.<sup>27,28</sup> Indeed, we found that SCF was an autocrine survival factor for BMdDCs with high c-kit expression, and that addition of exogenous SCF induced phospho-Akt increase, while total Akt remained unchanged.<sup>27</sup> Similarly, SCF counteracted the cell number decrease observed when purified spleen DCs were cultured *in vitro* for 2 days,<sup>28</sup> thus confirming the prosurvival role of this factor for mouse DCs.

Building on our previous work, in this report, we focused on mouse DCs in the steady state, demonstrating that spleen and BM DCs have a hypoxic phenotype, with some differences according to c-kit expression and cDC subset. We also investigated here the regulation of hypoxia-induced response and autophagy, two processes that are central to cellular homeostasis in hypoxic conditions, by the hematopoietic cytokine SCF, the only known ligand for c-kit.<sup>41</sup> Even though it has long been known that c-kit is normally expressed by mature cDCs in lymphoid organs,<sup>3</sup> its role in DC biology has been poorly investigated. This might be partly due to the fact that c-kit is

negatively regulated by GM-CSF, a typical supplement of DC culture medium,<sup>27</sup> and furthermore that c-kit is strongly downregulated upon DC activation by commonly used stimuli, such as CpG (bacterial 5'-Cytosine-phosphate-Guanine-3' DNA) and Poly I:C (Polyinosinic:polycytidylic acid) two synthetic products mimicking bacterial and viral nucleic acids, respectively, as well as by the proinflammatory cytokines TNF- $\alpha$  and IFN- $\beta$ .<sup>28</sup> Our results pointed to a regulatory role of SCF on hypoxia-induced response and autophagy.

In more detail, we showed here that mouse CD11c<sup>hi</sup> MHC-II<sup>hi</sup> DCs have a hypoxic phenotype in the spleen and BM, as demonstrated by their high expression of the transcription factor HIF-1 $\alpha$ , and their elevated labeling with PIM, a hypoxic marker. Remarkable differences in hypoxic phenotype were evident among different DC subsets. Indeed, we observed that c-kit<sup>+</sup> DCs had a significantly higher PIM MFI than c-kit<sup>-</sup> DCs in the spleen. Results were similar in the BM. Notably, HIF-1 $\alpha$  expression and PIM staining indicate a hypoxic state independently of distance from vessels, as previously demonstrated by elegant *in situ* tissue analysis.<sup>18</sup> To further investigate gene expression heterogeneity among spleen DCs with respect to hypoxic response, we exploited publicly available bulk RNAseq data generated by Alexander Rudensky's lab on three



different spleen cDC subsets, that is, T-bet<sup>+</sup> cDC2A, T-bet<sup>-</sup> cDC2B, and XCR1<sup>+</sup> cDC1.<sup>5</sup> We analyzed enrichment to annotation to the cellular pathway of response to hypoxia across genes showing higher expression levels in cDC2As or cDC2Bs and found a bias toward genes with higher expression in cDC2Bs. Similarly, when comparing annotation distribution as a function of gene expression in cDC2As versus cDC1s, there was a bias in the involvement in the cellular response to hypoxia for genes expressed at higher levels in cDC1s, whereas no significant difference was observed between cDC2Bs and cDC1s. We also analyzed publicly available scRNAseq data of mouse spleen DCs,<sup>5</sup> and found that the only cell cluster expressing *Kit* out of 18 clusters had a significant enrichment in genes implicated in oxygen sensing and hypoxia. Altogether, these results show that hypoxia-response pathways are activated in mouse spleen and BM DCs, with some differences among DC subsets, thus adding one layer of heterogeneity on top of already known diversities in DC subsets/phenotypes.

In vitro studies in normoxia showed that SCF/c-kit signaling increased HIF-1 $\alpha$  protein accumulation in pancreatic cancer cells and in HSCs,<sup>22,42</sup> and upregulated several hypoxia-responsive genes in HSCs,<sup>22</sup> suggesting that SCF enhances hypoxia response, at least in some cell types. Building on our previous findings on the SCF-triggered pathway in mouse DCs,<sup>27,28</sup> we performed gene expression microarray analysis of mouse BMdDCs cultured in hypoxia, and incubated either in the presence or absence of SCF. Using pathway enrichment analysis, we found that annotation to the response to hypoxia gene sets GO term 0071456 and 0001666 was significantly biased toward genes expressed at higher levels in the absence of SCF, suggesting that SCF addition modulated the response to low oxygen tension in our culture conditions. It should be highlighted that our experimental conditions are different from those of the above-cited studies on SCF-mediated upregulation of hypoxia-responsive genes<sup>22</sup> both with respect to cell types, that is, BMdDCs versus HSCs, and culture conditions, that is, hypoxia versus normoxia.

Increasing evidence supports the role of autophagy in immune cell biology and function.<sup>43</sup> For example, autophagy contributes to the elimination of intracellular pathogens and regulates antigen-presentation by DCs<sup>43,44</sup>; nevertheless, it can also favor viral replication and dampen immune response by degrading components of activatory pathways.<sup>45</sup> Similarly, autophagy can regulate either positively or negatively cell survival, depending on the intra- and extracellular context.<sup>46,47</sup> Autophagy is controlled by a complex interplay of molecular pathways. More specifically, it is jointly regulated by metabolic cues and immune receptor signals in macrophages and DCs.<sup>43,47,48</sup> We recently observed that oxygen tension has an impact on LPS-triggered autophagy in human monocyte-derived DCs.<sup>49</sup> We thus examined enrichment in a series of autophagy-related gene sets in BMdDCs stimulated with SCF in hypoxic conditions, and found that autophagy, autophagosome assembly, regulation of autophagy, and positive regulation of autophagy gene sets were all significantly biased toward genes expressed at higher levels in the absence of SCF, suggesting that in our culture conditions SCF counteracted homeostatic autophagy,

possibly reinforced under hypoxia.<sup>13</sup> Since autophagy has been involved in antigen presentation,<sup>43,44</sup> it might be expected that SCF modulates antigen presentation by DCs. However, in our previous study, SCF did not modulate MHC-I- nor MHC-II-restricted presentation of the soluble protein ovalbumin by mouse BMdDCs under normoxia,<sup>27</sup> suggesting that the impact of SCF on autophagy, and of autophagy on antigen presentation, might depend on oxygen tension and/or antigen type.

In short, our results show that mouse spleen and BM DCs are heterogeneous with respect to hypoxic phenotype, possibly reflecting intrinsic cellular differences, and/or diversities in tissue microenvironments. Furthermore, our in vitro findings suggest that SCF is involved in modulating DC response to hypoxia and inhibiting autophagy. Together with our previous demonstration that SCF acts as a prosurvival factor for DCs,<sup>27,28</sup> this study implicates SCF/c-kit in the regulation of DC homeostasis under physiological conditions. Our results might be relevant also for hypoxia and autophagy regulation in cancer.<sup>50-52</sup> For example, our findings might provide a new perspective on previous results showing that the presence of c-kit<sup>+</sup> DCs in tumor myeloid compartment correlated with favorable prognosis.<sup>53</sup>

#### ACKNOWLEDGMENTS

We thank Dr. Sara Vitale (Istituto Superiore di Sanità, Rome, Italy) for useful suggestions, Prof. Domenico Raimondo (Sapienza University, Rome, Italy), and Prof. Maria Foti (Bicocca University, Milan, Italy) for discussion and helpful inputs on bioinformatic analysis. This study was supported by the Italian Minister of Research and University (MIUR) grant PRIN 2017K55HLC (to F. D.), Consiglio Nazionale delle Ricerche (CNR) award CNR-STM 2019 and CNR-STM 2021 (to F.D.), and Italian Association for Cancer Research (AIRC) fellowship to M. L. (code 2020-25307). Open Access Funding provided by Consiglio Nazionale delle Ricerche within the CRUI-CARE Agreement.

#### CONFLICT OF INTEREST

The authors declare no conflict of interest.

#### DATA AVAILABILITY STATEMENT

The data that support the findings of this study are available in the supplementary material of this article. Microarray data are available in the public domain: GEO (GSE201172). Bulk RNAseq and scRNAseq data were derived from the following resources available in the public domain: GEO (GSE130201) and GEO (GSE137710)(1).

#### ORCID

Amarelys Belen Barroeta Seijas  <http://orcid.org/0000-0001-7538-4553>

Mattia Laffranchi  <http://orcid.org/0000-0002-0556-6068>

Francesca Di Rosa  <http://orcid.org/0000-0003-0252-9138>

#### REFERENCES

1. Granucci F, Zanoni I, Ricciardi-Castagnoli P. Central role of dendritic cells in the regulation and deregulation of immune responses. *Cell Mol Life Sci.* 2008;65:1683-1697.

2. Riboldi E, Musso T, Moroni E, et al. Cutting edge: proangiogenic properties of alternatively activated dendritic cells. *J Immunol.* 2005;175:2788-2792.
3. Merad M, Sathe P, Helft J, Miller J, Mortha A. The dendritic cell lineage: ontogeny and function of dendritic cells and their subsets in the steady state and the inflamed setting. *Annu Rev Immunol.* 2013;31:563-604.
4. Guillems M, Ginhoux F, Jakubzick C, et al. Dendritic cells, monocytes and macrophages: a unified nomenclature based on ontogeny. *Nat Rev Immunol.* 2014;14:571-578.
5. Brown CC, Gudjonson H, Pritykin Y, et al. Transcriptional basis of mouse and human dendritic cell heterogeneity. *Cell.* 2019;179:846-863.e24.
6. Alcántara-Hernández M, Leylek R, Wagar LE, et al. High-dimensional phenotypic mapping of human dendritic cells reveals interindividual variation and tissue specialization. *Immunity.* 2017;47:1037-1050.
7. Taylor CT, Colgan SP. Regulation of immunity and inflammation by hypoxia in immunological niches. *Nat Rev Immunol.* 2017;17:774-785.
8. Braun RD, Lanzen JL, Snyder SA, Dewhirst MW. Comparison of tumor and normal tissue oxygen tension measurements using OxyLite or microelectrodes in rodents. *Am J Physiol Heart Circ Physiol.* 2001;280:H2533-H2544.
9. Spencer JA, Ferraro F, Roussakis E, et al. Direct measurement of local oxygen concentration in the bone marrow of live animals. *Nature.* 2014;508:269-273.
10. Petrova V, Annicchiarico-Petruzzelli M, Melino G, Amelio I. The hypoxic tumour microenvironment. *Oncogenesis.* 2018;7:10.
11. Sitkovsky M, Lukashev D. Regulation of immune cells by local-tissue oxygen tension: HIF1 alpha and adenosine receptors. *Nat Rev Immunol.* 2005;5:712-721.
12. Nizet V, Johnson RS. Interdependence of hypoxic and innate immune responses. *Nat Rev Immunol.* 2009;9:609-617.
13. Fang Y, Tan J, Zhang Q. Signaling pathways and mechanisms of hypoxia-induced autophagy in the animal cells. *Cell Biol Int.* 2015;39:891-898.
14. Bosco MC, Varesio L. Dendritic cell reprogramming by the hypoxic environment. *Immunobiology.* 2012;217:1241-1249.
15. Mancino A, Schioppa T, Larghi P, et al. Divergent effects of hypoxia on dendritic cell functions. *Blood.* 2008;112:3723-3734.
16. Semenza GL. Hypoxia-inducible factors in physiology and medicine. *Cell.* 2012;148:399-408.
17. Scholz CC, Taylor CT. Targeting the HIF pathway in inflammation and immunity. *Curr Opin Pharmacol.* 2013;13:646-653.
18. Nombela-Arrieta C, Pivarnik G, Winkel B, et al. Quantitative imaging of haematopoietic stem and progenitor cell localization and hypoxic status in the bone marrow microenvironment. *Nat Cell Biol.* 2013;15:533-543.
19. Corcoran SE, O'Neill LAJ. HIF1 $\alpha$  and metabolic reprogramming in inflammation. *J Clin Invest.* 2016;126:3699-3707.
20. Rius J, Guma M, Schachtrup C, et al. NF-kappaB links innate immunity to the hypoxic response through transcriptional regulation of HIF-1alpha. *Nature.* 2008;453:807-811.
21. Tannahill GM, Curtis AM, Adamik J, et al. Succinate is an inflammatory signal that induces IL-1beta through HIF-1alpha. *Nature.* 2013;496:238-242.
22. Pedersen M, Lofstedt T, Sun J, Holmquist-Mengelbier L, Pahlman S, Ronnstrand L. Stem cell factor induces HIF-1alpha at normoxia in hematopoietic cells. *Biochem Biophys Res Commun.* 2008;377:98-103.
23. Jantsch J, Wiese M, Schodel J, et al. Toll-like receptor activation and hypoxia use distinct signaling pathways to stabilize hypoxia-inducible factor 1alpha (HIF1A) and result in differential HIF1A-dependent gene expression. *J Leukoc Biol.* 2011;90:551-562.
24. Filippi I, Morena E, Aldinucci C, Carraro F, Sozzani S, Naldini A. Short-term hypoxia enhances the migratory capability of dendritic cell through HIF-1alpha and PI3K/Akt pathway. *J Cell Physiol.* 2014;229:2067-2076.
25. Jantsch J, Chakravorty D, Turza N, et al. Hypoxia and hypoxia-inducible factor-1 alpha modulate lipopolysaccharide-induced dendritic cell activation and function. *J Immunol.* 2008;180:4697-4705.
26. Krishnamoorthy N, Oriss TB, Paglia M, et al. Activation of c-Kit in dendritic cells regulates T helper cell differentiation and allergic asthma. *Nat Med.* 2008;14:565-573.
27. Barroeta Seijas AB, Simonetti S, Vitale S, et al. GM-CSF inhibits c-Kit and SCF expression by bone marrow-derived dendritic cells. *Front Immunol.* 2017;8:147.
28. Simonetti S, Seijas ABB, Natalini A, et al. Dendritic cells modulate c-Kit expression on the edge between activation and death. *Eur J Immunol.* 2019;49:534-545.
29. Andreas N, Riemann M, Castro CN, et al. A new RelB-dependent CD117<sup>+</sup> CD172a<sup>+</sup> murine DC subset preferentially induces Th2 differentiation and supports airway hyperresponses in vivo. *Eur J Immunol.* 2018;48:923-936.
30. Chu CL, Lee YP, Pang CY, Lin HR, Chen CS, You RI. Tyrosine kinase inhibitors modulate dendritic cell activity via confining c-Kit signaling and tryptophan metabolism. *Int Immunopharmacol.* 2020;82:106357.
31. Roskoski RJ. Signaling by Kit protein-tyrosine kinase—the stem cell factor receptor. *Biochem Biophys Res Commun.* 2005;337:1-13.
32. Reber L, Da Silva CA, Frossard N. Stem cell factor and its receptor c-Kit as targets for inflammatory diseases. *Eur J Pharmacol.* 2006;533:327-340.
33. Jankovic B, Aquino-Parsons C, Raleigh JA, et al. Comparison between pimonidazole binding, oxygen electrode measurements, and expression of endogenous hypoxia markers in cancer of the uterine cervix. *Cytometry B Clin Cytom.* 2006;70:45-55.
34. Hao Y, Hao S, Andersen-Nissen E, et al. Integrated analysis of multimodal single-cell data. *Cell.* 2021;184:3573-3587.e29.
35. Stuart T, Butler A, Hoffman P, et al. Comprehensive integration of single-cell data. *Cell.* 2019;177:1888-1902.e21.
36. Hafemeister C, Satija R. Normalization and variance stabilization of single-cell RNA-seq data using regularized negative binomial regression. *Genome Biol.* 2019;20:296.
37. Raudvere U, Kolberg L, Kuzmin I, et al. g:Profiler: a web server for functional enrichment analysis and conversions of gene lists (2019 update). *Nucleic Acids Res.* 2019;47:W191-W198.
38. Sapozhnikov A, Pewzner-Jung Y, Kalchenko V, Krauthgamer R, Shachar I, Jung S. Perivascular clusters of dendritic cells provide critical survival signals to B cells in bone marrow niches. *Nat Immunol.* 2008;9:388-395.
39. Subramanian A, Tamayo P, Mootha VK, et al. Gene set enrichment analysis: a knowledge-based approach for interpreting genome-wide expression profiles. *Proc Natl Acad Sci USA.* 2005;102:15545-15550.
40. Pelayo R, Hirose J, Huang J, et al. Derivation of 2 categories of plasmacytoid dendritic cells in murine bone marrow. *Blood.* 2005;105:4407-4415.
41. Broudy VC. Stem cell factor and hematopoiesis. *Blood.* 1997;90:1345-1364.
42. Zhang M, Ma Q, Hu H, et al. Stem cell factor/c-kit signaling enhances invasion of pancreatic cancer cells via HIF-1alpha under normoxic condition. *Cancer Lett.* 2011;303:108-117.
43. Deretic V, Saitoh T, Akira S. Autophagy in infection, inflammation and immunity. *Nat Rev Immunol.* 2013;13:722-737.
44. Ho NI, Camps MGM, Verdoes M, Münz C, Ossendorp F. Autophagy regulates long-term cross-presentation by murine dendritic cells. *Eur J Immunol.* 2021;51:835-847.
45. Tao S, Drexler I. Targeting autophagy in innate immune cells: angel or demon during infection and vaccination. *Front Immunol.* 2020;11:460.

46. Doherty J, Baehrecke EH. Life, death and autophagy. *Nat Cell Biol.* 2018;20:1110-1117.
47. Wang Y, Zhang H. Regulation of autophagy by mTOR signaling pathway. *Adv Exp Med Biol.* 2019;1206:67-83.
48. Nouwen LV, Everts B. Pathogens MenTORing macrophages and dendritic cells: manipulation of mTOR and cellular metabolism to promote immune escape. *Cells.* 2020;9:E161.
49. Monaci S, Aldinucci C, Rossi D, et al. Hypoxia shapes autophagy in LPS-activated dendritic cells. *Front Immunol.* 2020;11:573646.
50. Schlie K, Spowart JE, Hughson LR, Townsend KN, Lum JJ. When cells suffocate: autophagy in cancer and immune cells under low oxygen. *Int J Cell Biol.* 2011;2011:470597.
51. Noman MZ, Janji B, Berchem G, Mami-Chouaib F, Chouaib S. Hypoxia-induced autophagy: a new player in cancer immunotherapy? *Autophagy.* 2012;8:704-706.
52. Fotalan D, Huang CT, Schmidt-Wolf IG, Larsson M, Messmer D. Effect of oxygen levels on the physiology of dendritic cells: implications for adoptive cell therapy. *Mol Med.* 2011;17:910-916.
53. Broz ML, Binnewies M, Boldajipour B, et al. Dissecting the tumor myeloid compartment reveals rare activating antigen-presenting cells critical for T cell immunity. *Cancer Cell.* 2014;26:638-652.

#### SUPPORTING INFORMATION

Additional supporting information can be found online in the Supporting Information section at the end of this article.

**How to cite this article:** Barroeta Seijas AB, Simonetti S, Filippi I, et al. Mouse dendritic cells in the steady state: hypoxia, autophagy, and stem cell factor. *Cell Biochem Funct.* 2022;40:718-728. doi:10.1002/cbf.3737